# On Symmetry and Anisotropy of Earth-core Flows

Nathanaël Schaeffer, Maria Alexandra Pais

# On Symmetry and Anisotropy of Earth-core Flows

N. Schaeffer[1] and M. A. Pais[2]

[1] *ISTerre, CNRS, University Joseph Fourier, BP 53, 38041 Grenoble Cedex 9, France.*
[2] *CFC, Physics Department, University of Coimbra, 3004-516 Coimbra, Portugal.*
(Dated: 6 april 2011, published in *Geophys. Res. Lett.*, doi:10.1029/2011GL046888)

Quasi-geostrophic (QG) flows are a recently developed and very promising paradigm for modeling decadal secular variation (SV). Here we examine the effects of allowing anisotropy and departures of the flow from quasigeostrophy. We perform dedicated numerical experiments of the flow dynamics and magnetic induction inside the Earth's liquid core at time scales characteristic of secular variation of the geomagnetic field. Obtained results motivate new flow inversion regularization featuring an equatorially anti-symmetric component superimposed to quasi-geostrophic columns, and stronger latitudinal than longitudinal flow gradients. Applying these constraints allows to explain the observed SV for the whole period 1840-2010, and most significantly, provides a clearly improvement in prediction for decadal length-of-day variations for the period 1980-2000. Furthermore, the trace of the inner-core appears clearly without any assumption for the 1997-2010 period covered by satellite geomagnetic data. Our results support QG being the appropriate description of the force balance within the core on decadal time scales and large spatial scales.

## I. INTRODUCTION

The secular variation of the magnetic field of the Earth is due to the flow of liquid metal advecting the magnetic field inside the Earth's core. A large number of studies have focused on inference of the core surface flow from geomagnetic field data [7]. Recently, it has been advocated that Quasi-Geostrophic (QG) flows should give a good description of the flow in the core [9], and kinematic properties of this type of flow have already been used to constrain the core surface flow models inferred from magnetic field data to be symmetric with respect to the equator and purely azimuthal at the rim of the tangent cylinder [4, 16].

Still, some unclear points persist, and our study tries to shed some light on three of them: (i) The QG hypothesis has been justified for asymptotically small slopes (e.g. [11]), and the question arises as to its validity in the vicinity of the equator of both inner core and core-mantle boundary. For example, a flow crossing the equator line, like under the Indian ocean and Brazil in models where the tangential geostrophy of flows was not imposed [14], could not be captured by a QG model, which imposes a purely azimuthal flow at the equator. (ii) Even though the global amount of equatorial symmetry of core surface flow models has been in general increasing with time during the period 1840-2010 [6], no analysis has been made to identify which are the spatial features that can be associated to QG dynamics. (iii) Recent efforts have been made to also take into account the uncertainties due to the advection of an unknown small scale geomagnetic field by an unresolvable small scale flow [3, 16]. However, these small scales are poorly constrained [4] and no useful information has been obtained from them. Underparameterization of core flow models due to regularizations penalizing too strongly small length scales may be the cause of the overestimation of decade length of day variations ($\Delta$LOD) seen in most studies. We investigate the possibility that this may be due to aliasing of small scales (which do not carry angular momentum in the model we use [10]) to large scales, by comparing estimations using different regularizations.

The paper is organized as follows. Section II presents results of direct numerical simulations which serve as motivation to propose new core surface constraints in section III. Specific features of our flow inversion are also stated there. The resulting core surface flow models are examined in section IV and compared with previously published models by testing their ability in estimating $\Delta$LOD. The mean flow model computed from CHAOS-3 is examined. A summary of our findings is presented in the Conclusion.

## II. DIRECT NUMERICAL SIMULATIONS

In order to gain insight into the kinematics of the flow inside the Earth core, we run full three dimensional numerical simulations in a spherical shell of radius $a$, rotating at period $T = 2\pi/\Omega$, and with a solid inner core of radius $0.35a$. The conducting fluid of density $\rho$, viscosity $\nu$ and magnetic diffusivity $\eta = \nu$ is permeated by a constant, toroidal and axisymmetric magnetic field $\mathbf{B}_0 = B_0 \nabla\times(4r(a-r)\mathbf{r}/a^3)$, with $B_0$ such that the Lehnert number $\lambda = B_0(\sqrt{\mu_0\rho}a\Omega)^{-1}$ (the ratio of the Alfvén wave to the inertial wave speeds) is set to $10^{-3}$, close to its value inside the Earth's core. A small $\lambda$ is important to resolve propagating inertial and Alfvén waves, both having a crucial role on SV dynamics [9]. We solve the Navier-Stokes equation (including the Coriolis and Lorentz force) together with the induction equation. The Ekman number $E = \nu(a^2\Omega)^{-1}$ is set to $10^{-6}$ and we use stress-free boundaries. The mantle and the inner-core are insulators in these calculations, although the boundary condition has no visible impact on the geometry of the flow. Details about the code can be found in [6].

The simulation is performed in two steps. First, from a state of rest, we impose a localized bulk

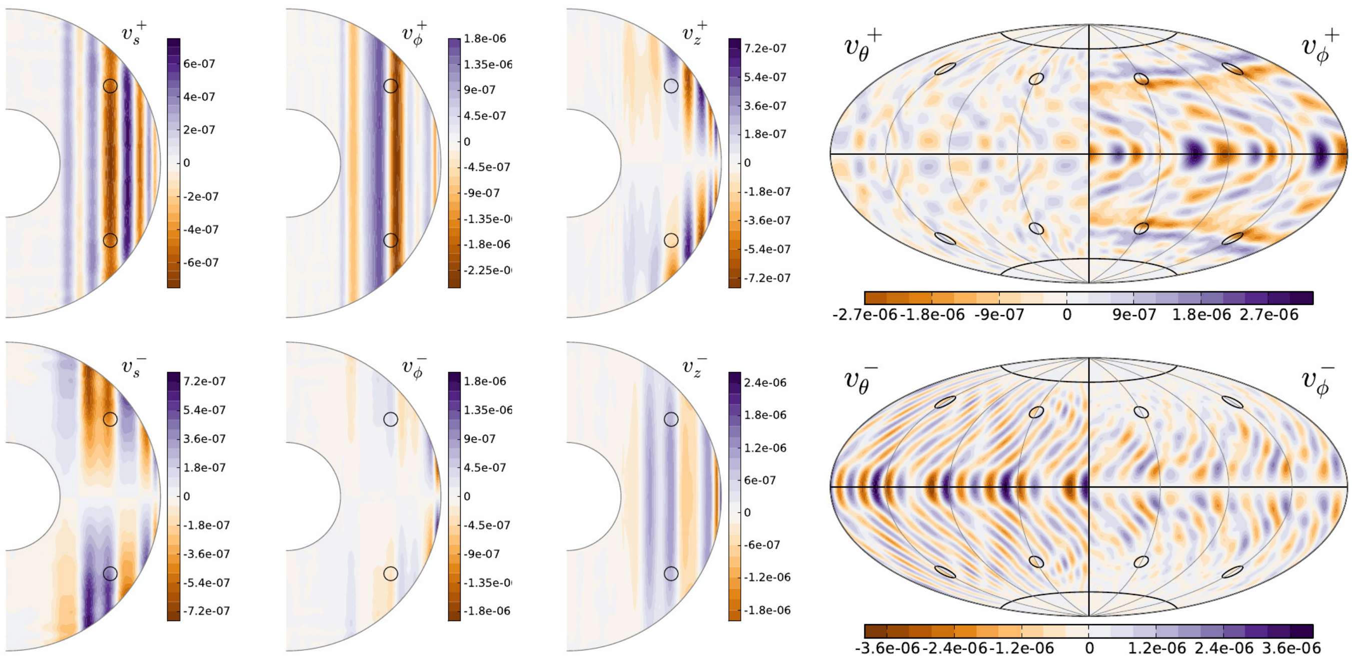


FIG. 1. Flows resulting from a symmetric (top) or anti-symmetric (bottom) forcing followed by $110T$ of free decay. From left to right: the cylindrical components ($v_s$,$v_\phi$,$v_z$) in the meridional plane containing $\mathbf{r}_\pm$, and the spherical components ($v_\theta$,$v_\phi$) at the core-surface (note on the right the use of a 4-fold symmetry in the simulation). The circles indicate the location of the applied forcing in the meridian plots, and its projection along the $z$-axis on the surface plots. The surface projection of the equator of the inner-core is also drawn. Velocities are expressed in units of $a\Omega$.

force field $\mathbf{F}^\pm(\mathbf{r}) = F_0 \nabla \times [\mathbf{r}\exp(-|\mathbf{r}-\mathbf{r}_+|^2/\delta^2) \pm \mathbf{r}\exp(-|\mathbf{r}-\mathbf{r}_-|^2/\delta^2)]$, where $\mathbf{r}_\pm = (0.675a, \pi/4, \pm a/2)$ in cylindrical coordinates $(s,\phi,z)$ with origin $O$ in the center of the sphere, and $Oz$ parallel to the global rotation axis. The forcing length-scale is set to $\delta = 0.045a$, while its amplitude $F_0$ is chosen so that the resulting flow $\mathbf{v}$ is of low amplitude : $v \ll a\Omega$. After a duration $\Delta t = 6T$ allowing for the formation of Taylor columns through the propagation of inertial waves, we stop the forcing and let the flow freely decay during the second step of the simulation.

Figure 1 shows the flow after 110 periods of free decay, in the two forcing cases: either symmetric ($\mathbf{F}^+$) or anti-symmetric ($\mathbf{F}^-$) with respect to the equator. We observe that these flows have undistinguishable decay rates. As expected for low values of $\lambda$, the symmetric forcing leads to a flow $\mathbf{v}^+$ that is nearly QG: $v_s^+$, $v_\phi^+$ are independent of $z$, satisfying the Taylor-Proudman (TP) constraint $\partial_z \mathbf{v} = 0$, while $v_z^+ \propto z$ ensures the impermeability of the boundaries. The anti-symmetric flow $\mathbf{v}^-$ is certainly less known: $v_z^-$ satisfies the TP constraint but induces $v_s^-$ and $v_\phi^-$ that do not, in order to ensure the impenetrability of the boundaries. Furthermore, it appears that $\mathbf{v}^+$ is dominated by $v_\phi^+$ and a tendency to zonation, while $\mathbf{v}^-$ has higher values at large $s$ or low latitude, where it is dominated by $v_z^-$ (or $v_\theta^-$). The increasingly large boundary slope when $s \to 1$ reduces the amount of $v_s^-$ produced by $v_z^-$ at the boundaries. Finally, in spite of a localized forcing, both $\mathbf{v}^+$ and $\mathbf{v}^-$ tend to spread over the whole volume outside the cylinder tangent to the inner-core equator (TC). We obtain similar results when replacing the toroidal forcing $\mathbf{F}^\pm$ with a poloidal one, except for $v_z^-$ which is weaker and has a more complex dependence on $z$.

## III. PROPOSED CONSTRAINTS FOR INVERTING THE CORE FLOW AND METHODOLOGY

We propose to translate the results obtained for $\mathbf{v}$ in the previous section to surface core flows $\mathbf{u}$ which can be computed from geomagnetic field models. The $\mathbf{v}^+$ QG flow (also referred to as a columnar flow) leads to the following relation at the core surface [1] :

$$\nabla_H \cdot \mathbf{u}^+ = 2u_\theta^+ \tan\theta \qquad (1)$$

The axial component of the $\mathbf{v}^-$ flow comprises, besides a z-invariant term, other anti-symmetric contributions that cannot be separated at the core surface. This precludes the derivation of a kinematic constraint for $\mathbf{u}^-$. We will thus invert for flows that, besides a symmetric component $\mathbf{u}^+$ satisfying (1), will also include an antisymmetric component $\mathbf{u}^-$ which has no particular kinematical constraint imposed.

In the Earth core, due to the very small viscosity and high electrical conductivity, we do not expect any significant damping effect on the flow at the scales that can be probed by magnetic field models. However, observations and numerical results for different natural rotating flow systems, with or without magnetic fields, show a tendency for the flow to develop preferably along parallels, in the form of thin zonal jets. This leads to anisotropic structures elongated in the azimuthal direction but showing small scales in the radial direction. The most emblematic case is the banded atmosphere of Jupiter, but there is also evidence for alternating jets in the Ocean [12]. Numerical simulations of thermal convection also exhibit this kind of flow [2] and recent geodynamo simulations by [13] show the formation of low-latitude zonal flows at low Ekman numbers. Inspired by these results, we propose a penalization of the azimuthal gradients, by minimizing the integral over the core-mantle surface (CMB):

$$R_A = \int_{\mathrm{CMB}} \left[ \frac{1}{\sin\theta} \frac{\partial \mathbf{u}}{\partial \phi} \right]^2 dS. \qquad (2)$$

This anisotropic norm can be shown to depend both on spherical harmonic degree $\ell$ and order $m$ as $\ell m^2$. Because it does not restrain zonal flows (and hence torsional oscillations), we superimpose an isotropic penalization of the mean squared velocities over the core surface ($\int_{\mathrm{CMB}} \mathbf{u}^2 dS$, referred to as $\ell^1$ norm).

To cover a time interval as large as possible and treat different geomagnetic field models, we invert the gufm1 [8], the comprehensive CM4 [17] and the satellite derived CHAOS-3 [15] geomagnetic field models up to degree $\ell = 13$. We obtain snapshots of core surface fluid flow up to $\ell = 26$ that can, by advecting the field, explain the secular variation models (frozen-flux hypothesis). The adopted methodology is described in [7]. We look for a regularized weighted least squares flow solution that explains snapshots of the geomagnetic field model up to some degree of confidence, which comprises both the information on the noise level of the SV data ($\sigma^d(\ell)$) and an estimation of the SV signal produced by a non-parameterized contribution of the magnetic field small scales (representativity error, $\sigma^r(\ell)$) [4]. Assuming these two kinds of errors are uncorrelated, we then construct a diagonal predictive data covariance matrix with elements $\sigma^d(\ell)^2 + \sigma^r(\ell)^2$. The term representing the confidence on the SV model, $\sigma^d(\ell)^2$, is given by $\eta(2\ell+1)^{-1}(\ell+1)^{-1}$, where we use as noise level $\eta$ the value 0.4 $(\mathrm{nT/yr})^2$ for gufm1 and CM4 models (assuming that SV degrees $\ell < 10$ contain relevant information in both these models [5]), and 0.01 $(\mathrm{nT/yr})^2$ for the satellite derived model CHAOS-3 [15]. The representativity errors are assumed to be independent of time and we use the law $\sigma^r(\ell)^2 = 36\exp(-\ell)$, close to those derived by [16] and [4].

The inversion is stabilized using regularization presented above.Condition (1) is converted into a quadratic norm that is introduced in the global objective functional to be minimized by the flow solution. This condition constrains only but $\mathbf{u}^+$ using a very high Lagrange multiplier. We test the relevance of $\mathbf{u}^-$ by also inverting for purely symmetric flows that obey condition (1). Norm $R_A$ (eq. 2) is used to introduce anisotropy, in conjunction with the isotropic $\ell^1$ norm. To compare with more standard procedures where stronger regularizations are used, we also invert for flows using only an $\ell^3$ norm, which penalizes the mean squared velocity gradients over the CMB [4].

In order to test the sensitivity of geomagnetic field models to the boundary of the TC, we use the same regularizations over the whole core surface.

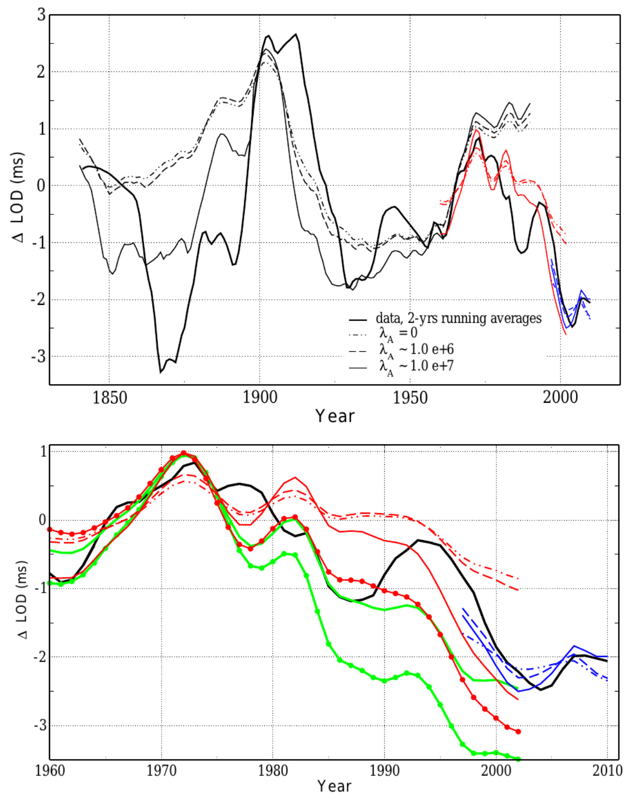


FIG. 2. Observed (thick black line) and estimated $\Delta$LOD. Top: estimates for gufm1 (thin black lines), CM4 (red) and CHAOS-3 (blue), for 3 different degrees of flow anisotropy. Bottom: blow up of top figure for the most recent period. Also shown, for CM4, estimates from large-scale $\mathbf{u}^+$ (green line with circles), small-scale $\mathbf{u}^+$ (green line) and large scale $\mathbf{u}^\pm$ (red line with circles).

## IV. INVERTED FLOW MODELS

The new regularizing norms are tested for a possible improvement of estimates of $\Delta$LOD. We concentrate on the 1960-2002 epoch covered by the CM4 model, for which the imposed anisotropy is responsible for the most clear improvement. It is known that standard flow predictions do recurrently introduce a stronger decaying

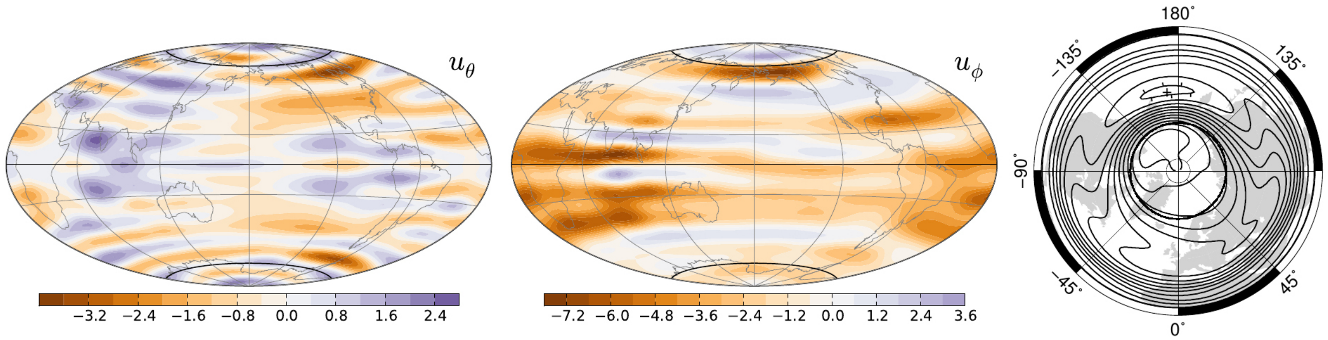


FIG. 3. Inverted flow $\bar{\mathbf{u}}^{\pm}$ using $\lambda_A = 8 \times 10^6$ averaged over the CHAOS-3 era. From left to right : $u_\theta$ and $u_\phi$ components in km/yr, and the stream-function $\xi$ of the symmetric part $\bar{\mathbf{u}}^{+}$ viewed from north-pole defined by $\bar{\mathbf{u}}^{+} = (\cos\theta)^{-2}\, \mathbf{r} \times \nabla\xi$. The parallel coresponding to the trace of the TC is drawn (as well as $\pm 20°$, related to table IV).

trend of ΔLOD than observed during this period [4]. We test the hypothesis that this poor estimation may be due to aliasing caused by underparameterization of small scales. This would deteriorate estimation of large scale coefficients, in particular $t_1^0$ and $t_3^0$ (which carry the core angular momentum) and more importantly deteriorate the accuracy of their time variations. In figure 2 we show estimates produced by $\mathbf{u}^+$ flows and flows supporting an equatorial antisymmetric component besides the QG symmetric one ($\mathbf{u}^{\pm}$ flows), with different small scale penalization strength. The ΔLOD predicted by a large scale $\mathbf{u}^+$ flow model produces a too strong negative trend (normalized squared misfit $\chi^2 = 1.2$). When using a weaker regularization the results are clearly improved ($\chi^2 = 0.7$). But the best result is obtained when allowing for $\mathbf{u}^-$ and imposing lower longitudinal gradients ($\chi^2 = 0.55$).

We further check the importance of norm $R_A$ in improving the estimations. In figure 2 we show estimations for different degrees of anisotropy, quantified by different values of the regularizing parameter $\lambda_A$ weighting $R_A$: from $\lambda_A = 0$ (only the $\ell^1$ norm is used) to the maximum degree of anisotropy achieved while still explaining the SV model to a reasonable level. We note that using solely the isotropic regularization $\ell^1$ produces too low amplitude estimations, and that increasing the anisotropy constraint (and decreasing the isotropic one) improves the results. This is because the flow energy can be more freely distributed among different length-scales of the zonal flow coefficients, including those contributing to the core angular momentum.

We quantify the maximum anisotropy imposed on flow models computing $\alpha = (R_A^0 - R_A^*)/R_A^0$, where $R_A^0$ and $R_A^*$ are values of $R_A$ computed respectively for flows inverted with $\lambda_A = 0$ (no anisotropy) and for the maximum achieved $\lambda_A$. We find $\alpha$ increasing from 0.8 to 0.9 during the 1840-2010 period. The good recovery of the trend and the amplitude of oscillations in ΔLOD is not specific to inversions of CM4, and we show in figure 2 the good results obtained for gufm1 (1840-1990) and CHAOS-3 (1997-2010).

We proceed to identify the core surface regions where

| $\ell_{tr}$ | 6 | 10 | 13 | 18 | 26 |
|---|---|---|---|---|---|
| core surface | 0.84 | 0.80 | 0.76 | 0.70 | 0.66 |
| inside TC | 0.63 | 0.79 | 0.38 | 0.27 | 0.22 |
| equator | 0.91 | 0.91 | 0.83 | 0.67 | 0.65 |

TABLE I. Ratio of symmetric kinetic energy over total energy $E^+/(E^+ + E^-)$ for the flow $\bar{\mathbf{u}}^{\pm}$ (fig. 3) truncated at different spherical harmonic degree $\ell_{tr}$ and integrated over the whole core surface, inside the TC, and also over a band centered on the equator and spanning 40° of latitude.

the $\mathbf{u}^-$ component is more important, as accounted by SV models in the frozen-flux approximation. We concentrate on the more recent CHAOS-3 model (derived from very recent satellite data and revised observatory monthly mean values) and compute the corresponding mean anisotropic flow model $\bar{\mathbf{u}}^{\pm}$, represented in figure 3. Its rms velocity is 9.7 km/yr during the 1997-2010 period. We note the important contribution of $u_\theta^-$ in the equatorial region, where the crossing of the equator under Indonesia is quite obvious. However, only small scales are affected by the breakdown of QG near the equator, while the large scale flow remains highly symmetric outside the TC (see table 1). Most striking is the sharpness with which the $\bar{\mathbf{u}}^+$ flow model perceives the inner-core, as shown by its streamfunction ($\xi$, fig. 3 right).

## V. CONCLUSION

Our direct numerical simulations show that for short time-scale symmetric forcing, the flow response is quasi-geostrophic in Earth's core conditions. For an anti-symmetric forcing, an anti-symmetric counterpart of the QG flow could account for flows crossing the core-mantle boundary equator. As this component seems to decay at the same rate as the QG component, we argue that the presence of anti-symmetric flows at the core surface depends mainly on the amount of anti-symmetric forcing (whether buoyant, turbulent or magnetic) in the Earth core. Our simulations also show the development of longitudinal structures for the symmetric part, and a clear separation between the regions inside and outside the tangent cylinder. These results have inspired new constraints that we used for inverting the flow at the core surface from geomagnetic field models.

Our flow models, with improved estimations of ΔLOD and the natural emergence of symmetric large scale features including the trace of the tangent cylinder, support three main implications : (i) the large scale flow in the Earth core responsible for SV is very likely dominated by QG motions; (ii) significant deviations to QG are expected for smaller scales and in the equatorial region; (iii) SV models seem to detect anisotropic flows in the Earth core, with zonation and strong latitudinal gradients.

**ACKNOWLEDGMENTS**

We would like to thank Dominique Jault and Nicolas Gillet for fruitful discussions, and Nils Olsen for kindly sending us the CHAOS-3 main field coefficients. This research work was made possible by a joint FCT/CNRS grant. The simulations were run at the Service Commun de Calcul Intensif de l'Observatoire de Grenoble (SCCI).

[1] Amit, H., and P. Olson (2004), Helical core flow from geomagnetic secular variation, *Phys. Earth Planet. Inter.*, *147*, 1–25.
[2] Christensen, U. R. (2002), Zonal flow driven by strongly supercritical convection in rotating spherical shells, *Journal of Fluid Mechanics*, *470*, 115–133.
[3] Eymin, C., and G. Hulot (2005), On core surface flows inferred from satellite magnetic data, *Phys. Earth Planet. Inter.*, *152*, 200–220.
[4] Gillet, N., M. A. Pais, and D. Jault (2009), Ensemble inversion of time-dependent core flow models, *Geochemistry Geophysics Geosystems*, *10*(6), Q06,004+, doi: 10.1029/2008GC002290.
[5] Gillet, N., V. Lesur, and N. Olsen (2010), Geomagnetic core field secular variation models, *Space Science Reviews*, *155*(1), 129–145, doi:10.1007/s11214-009-9586-6.
[6] Gillet, N., N. Schaeffer, and D. Jault (2011), Rationale and geophysical evidence for quasi-geostrophic rapid dynamics within the Earth's outer core, *Phys. Earth Planet. Inter.*, *in press*, doi:10.1016/j.pepi.2011.01.005.
[7] Holme, R. (2007), *Large Scale Flow in the Core. In: Treatise in Geophysics, Geomagnetism, Vol. 8, pp107–129*, eds. P. Olson.
[8] Jackson, A., A. Jonkers, and M. Walker (2000), Four centuries of geomagnetic secular variation from historical records, *Phil. Trans. R. Soc. Lond. A*, *358*, 957–990.
[9] Jault, D. (2008), Axial invariance of rapidly varying diffusionless motions in the earth's core interior, *Physics of the Earth and Planetary Interiors*, *166*(1-2), 67–76, doi: 10.1016/j.pepi.2007.11.001.
[10] Jault, D., C. Gire, and J. L. Le Mouel (1988), Westward drift, core motions and exchanges of angular momentum between core and mantle, *Nature*, *333*(6171), 353–356, doi:10.1038/333353a0.
[11] Jones, C. A. (2007), *Thermal and compositional convection in the outer core. In: Treatise in Geophysics, Core Dynamics, Vol. 8, pp131–185*, eds. P. Olson, Amsterdam.
[12] Maximenko, N. A., B. Bang, and H. Sasaki (2005), Observational evidence of alternating zonal jets in the world ocean, *Geophys. Res. Lett.*, *32*, L12,607, doi: 10.1029/2005GL022728.
[13] Miyagoshi, T., A. Kageyama, and T. Sato (2010), Zonal flow formation in the earth's core, *Nature*, *463*(7282), 793–796, doi:10.1038/nature08754.
[14] Olsen, N., and M. Mandea (2008), Rapidly changing flows in the earth's core, *Nature Geoscience*, *1*, 390–394.
[15] Olsen, N., M. Mandea, T. J. Sabaka, and L. Tffner-Clausen (2010), The chaos-3 geomagnetic field model and candidates for the 11th generation igrf, *Earth Planets and Space*, *62*, 719–729, doi:10.5047/eps.2010.07.003.
[16] Pais, M. A., and D. Jault (2008), Quasi-geostrophic flows responsible for the secular variation of the earth's magnetic field, *Geophysical Journal International*, *173*(2), 421–443, doi:10.1111/j.1365-246X.2008.03741.x.
[17] Sabaka, T. J., N. Olsen, and M. E. Purucker (2004), Extending comprehensive models of the Earth's magnetic field with Ørsted and CHAMP data, *Geophys. J. Int.*, *159*, 521–547.